A biologically inspired model based on a multi-scale spatial representation for goal-directed navigation

Weilong Li[1], Dewei Wu[1], Jia Du[1,2] and Yang Zhou[1]

[1] Information and Navigation College, ,
Xi'an 710049, Shaanxi - P. R. China
[e-mail: weilongli2008@126.com]
[2] Xi'an Communications Institute,
Xi'an 710106, Shaanxi - P. R. China
*Corresponding author: Weilong Li

Received September 9, 2016; revised December 7, 2016; accepted January11, 2017; published March 31, 2017

Abstract

Inspired by the multi-scale nature of hippocampal place cells, a biologically inspired model based on a multi-scale spatial representation for goal-directed navigation is proposed in order to achieve robotic spatial cognition and autonomous navigation. First, a map of the place cells is constructed in different scales, which is used for encoding the spatial environment. Then, the firing rate of the place cells in each layer is calculated by the Gaussian function as the input of the Q-learning process. The robot decides on its next direction for movement through several candidate actions according to the rules of action selection. After several training trials, the robot can accumulate experiential knowledge and thus learn an appropriate navigation policy to find its goal. The results in simulation show that, in contrast to the other two methods(G-Q, S-Q), the multi-scale model presented in this paper is not only in line with the multi-scale nature of place cells, but also has a faster learning potential to find the optimized path to the goal. Additionally, this method also has a good ability to complete the goal-directed navigation task in large space and in the environments with obstacles.

Keywords: Place cells, Q-learning, spatial cognition, goal-directed navigation

This work has been supported by the National Natural Science Foundation of China under Grant No.61273048 and No.61473308.

https://doi.org/10.3837/tiis.2017.03.013 **ISSN : 1976-7277**

1. Introduction

Animals have a unique capability for autonomous navigation, which relies on complex and robust brain structures [1][2]. The hippocampus, as an important component of the brain, plays a crucial role in spatial cognition and navigation [3]. It can form an internal map to characterize spatial locations through the integration of allothetic and idiothetic information and take advantage of the accumulated experience to plan a reasonable route to the goal. As early as 1948, Tolman proposed the theoretical concept of a 'cognitive map' [6]. He found that a rat can form an internal map in its brain to encode its space and use the cognitive map to estimate its position in the environment. Two decades later, O'Keefe confirmed the existence of the spatial cognitive map and made the discovery of place cells in the rat hippocampus through an electrophysiological method [7][8]. The region corresponding to where the cells fire is called the 'place field' or 'firing field' [9]. Subsequently, head direction cells[10][11], grid cells [12][13], boundary cells [14], and speed cells [15] were discovered, which further revealed the mechanisms of biological navigation. The combination of these cells forms a compact 'navigation system' in the brain, which functions like a precise GPS. This system provides real-time spatial navigation information and guides the animal to its goal [16][17].

The study of various navigation cells in the brain and the important achievements in the fields of brain science and life sciences are interesting resources for researchers working on solving practical problems in navigation. Currently, there are many researchers working in this area [18]. From these studies we know that the progress of brain science is affecting the direction of development in navigation technology and it is feasible to solve these navigation problems by making use of the discoveries in the field of brain science. However, the above-mentioned references on building a model of spatial representation are based on a single scale of place cells. The latest research data shows that position in space is determined through a comprehensive characterization of multi-scale place cells in the hippocampus [24][25]. Therefore, a multi-scale spatial representation is more in line with the biological basis and is better equipped to deal effectively with the perceptual information from the spatial environment.

The work in [26] presents a spatial representation model based on forward planning of trajectories. The network of head direction cells, grid cells, and place cells is constructed to cognitively represent the conversion of information. The simulations and experiments show that the model can succeed in finishing a goal-directed navigation task and reduce the demand on the distance of the linear look-ahead trajectory. But this method mainly focuses on forming a map of the place cells and processing the information conversion, and it does not consider environments with obstacles. Ref. [27] introduces visual pretreatment technology and learning mechanisms into a bio-inspired system of a multi-scale map, which greatly improves the performance of position recognition. However, this model builds a relationship between the position units using supervised learning, which does not accord with the learning mechanism of biological brain navigation.

In this paper, we focus on the multi-scale nature of place cells in the hippocampus and the learning mechanisms of the brain. In order to complete a goal-directed navigation task, a bio-inspired spatial cognitive model based on a multi-scale place cell map is proposed. The Gaussian function is used to imitate the firing activity of a place cell. A multi-scale place cell map is constructed to encode the spatial environment. Then, a Q-learning algorithm is introduced to realize action selection. The robot can integrate the action activities from

different layers to decide on its next movement direction. The performance of the model is evaluated during a goal-directed robot navigational task. After several exploration trials, the robot is able to improve its understanding of the environment and succeed in finding an optimal path to the goal. The object of our study is the ground mobile robot and the method is also applicable for the unmanned vehicle.

This paper presents the following major contributions:

1. We build a multi-scale place cell map for spatial representation. The position of the agent is represented by the firing place cells in the different layers, which is not only in line with the multi-scale nature of place cells in the hippocampus, but also shows an exact and comprehensive description of the location.
2. We propose an improved Q-learning algorithm by introducing the activity factor into the multi-scale place cell map for goal-directed navigation. Through exploration and learning, the agent can plan an optimal route from the starting point to the goal. Additionally, the method is also feasible and effective in large spaces and in the environments with obstacles.
3. We compare the proposed method with two other methods (G-Q, S-Q) through extensive simulations, which demonstrate that our method has a faster learning speed in completing the goal-directed navigational task.

The rest of this paper is organized as follows. Section 2 describes a bio-inspired spatial cognitive model based on a multi-scale place cell map. Section 3 presents how the method performed in finishing a goal-directed navigational task. Section 4 provides conclusions and a discussion of future work.

2. A bio-inspired spatial cognitive model

The firing fields of place cells present different sizes along the dorso-ventral axis in the hippocampal formation. The dorsal firing field has a smaller scale and higher spatial recognition which can reflect the correct location of the robot. The ventral firing field has a larger scale and lower spatial recognition which can reflect a comprehensive description of the whole space [28]. Thus, we propose combining the advantages of the different scales into a bio-inspired spatial cognitive model based on a multi-scale place cell map. First, we introduce the firing model of a place cell and the Q-learning algorithm, and then we highlight the goal-directed navigation based on the improved Q-learning.

2.1 The firing model of a place cell

O'Keefe found that the activities of place cells in the rat hippocampus were closely related to its location in the environment [29]. Whenever the rat was in a particular place, some neural cells were activated. This special electrical activity could help the rat determine its position in the current environment. A single place cell corresponds with a concrete location region. Furthermore, a particular environment can be characterized by the electrical activities of a number of place cells. Ref.[9] shows that a majority of the place cells are located in the CA3 and CA1 areas of the hippocampus and they typically fire in a restricted portion of the environment. **Fig. 1** shows a response diagram of the place cells firing in CA3 and CA1 during an experiment. It can seen that there are some place cells that fire corresponding to the rat moving within its environment and the shape of the firing field is similar to a circle. Additionally, the intermediate regions of the firing cells have in turn a maximum response while decreasing outwards.

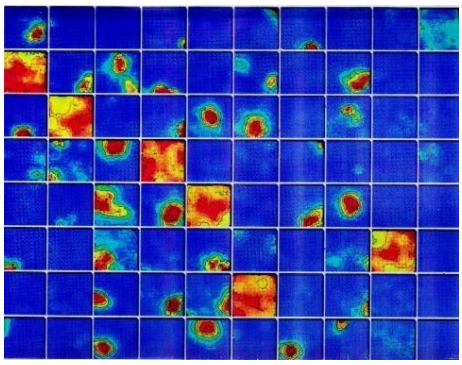

Fig. 1. A response diagram of the firing of hippocampal place cells[9]

According to the shape of the firing field, we can use the Gaussian function to imitate the place cell firing pattern. Let $\mathbf{p}$ be the current position of the robot, and the firing rate of the place cell i can be defined by:

$$PC_i(\mathbf{p}) = \exp\left(-\frac{\|\mathbf{p}-\mathbf{p}_0\|^2}{2\sigma^2}\right) \tag{1}$$

where $\mathbf{p}_0$ is the reference position of PC_i and σ is the adjustable factor of the firing field. **Fig. 2** shows the distribution of a place cell firing while $\sigma^2 = 30$. From the figure, it can be seen that the simulated place cell has a maximum response in the intermediate red area where the firing rate in the center is equal to 1, and the firing rate in the external blue color area is close to 0. Therefore, Eq.(1) is able to simulate the characteristics of the hippocampal place cell to some extent.

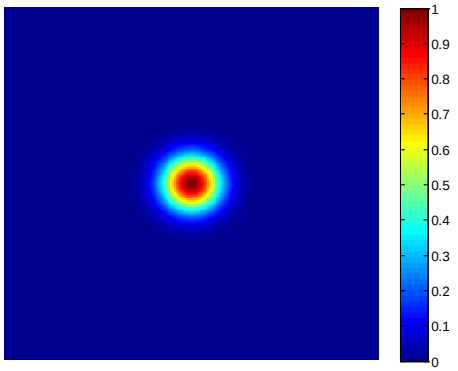

Fig. 2. A schematic diagram of a simulated place cell

2.2 Q-learning algorithm

Q-learning is one of the reinforcement learning algorithms which is usually used for path planning in the condition of no prior knowledge [30]. The algorithm first initializes a table of Q values, and adopts a greedy approach to pick an action. Then it updates the corresponding Q values according to feedback from a reward. Through several episodes, the action tends to the optimal behavior. The purpose of Q-learning is to estimate the Q value under the optimal policy on the premise that the transferred probability of the state is unknown. $Q(s_t, a_t)$

represents the function of performing an action in state s_t which can be expressed as Eq.(2):

$$Q(s_t, a_t) = r(s_t, a_t) + \gamma \max_{a_{t+1}} Q(s_{t+1}, a_{t+1}) \tag{2}$$

where $r(s_t, a_t)$ is the immediate reward from s_t to s_{t+1} by action a_t, and γ is the discount factor, $\gamma \in [0,1)$.

In the learning process, $Q(s_t, a_t)$ updates according to Eq.(3):

$$Q(s_t, a_t) = Q(s_t, a_t) + \eta\left(r(s_t, a_t) + \gamma \max_{a_{t+1}} Q(s_{t+1}, a_{t+1}) - Q(s_t, a_t)\right) \tag{3}$$

where η is the learning rate which controls the speed of learning. The greater value η will bring about a faster convergence. However, too large value η may cause premature convergence. Thus, it is important for the learning speed to choose a proper η.

2.3 The multi-scale spatial representation for goal-directed navigation based on Q-learning

2.3.1 Construction of the multi-scale place cell map

The place cell firing is mainly derived from two sources: one is the external sensory information, such as visual information, which takes the similarities between the current view and the origin view as the value of the firing rate [31]; the second source is self-motion information, such as speed and direction, which drives the place cells firing by path integration [32]. This paper focuses on how to use the firing effect from the different place cell scales to represent the position of the robot in the environment and initiate a reasonable action. Thus, the Gaussian model introduced in Section 2.1 is adopted to calculate the firing rate of the place cell in the subsequent analysis process. Namely, we use the concrete position information to directly drive the place cell firing instead of matching the local views or using path integration.

Suppose the moving area for the robot in its environment is covered by a $a \times a$ square and the place cells are built uniformly at a certain interval. As the place fields overlap, several cells might be firing at any given moment. Therefore, any position of the robot in the space can be characterized by a set of corresponding place cells in the firing state.

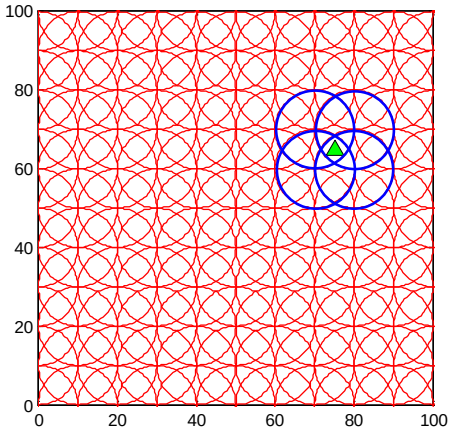

Fig. 3. A schematic diagram of the place cell map in a layer

By adjusting the size of the place field we can achieve a place cell map with different scales where the scale represents the corresponding layer. The firing rate of the place cell i in the layer l is expressed as:

$$PC_{il}(x,y)=\exp\left\{-\frac{(x-x_{il})^2+(y-y_{il})^2}{2\sigma^2}\right\} \tag{4}$$

where (x,y) represents the real position of the robot and (x_{il},y_{il}) represents the center of the place cell i in the layer l, and σ is the adjustable factor of the firing field.

Fig. 3 shows a schematic diagram of the place cell map in a layer in which the red circles indicate the constructed place cells, the green triangle indicates the robot, and the blue circles indicate the place cells in a firing state. From the figure, it can be seen that there are four place cells firing at the current location. Additionally, we can find corresponding place cells firing in other layers. Thus, the position of the robot in the space is synthetically characterized by the firing place cells in the different layers.

2.3.2 Q-learning on place cells

For the place cell map constructed in each layer, the firing rate of the place cell in the current state $PC_{il}(x,y)$ is calculated by Eq.(4). Considering that there may be several place cells firing at the same time, we define s_i as the state of the i th place cell and $act(s_i)$ as the activation value of state s_i which represents the probability state s_i in its current location. Then a greedy approach is adopted in Eq.(6) to choose an action, and the Q value is updated according to Eqs.(7) and (8).

$$act(s_i)=\frac{PC_{il}(x,y)}{\sum_{i=1}^{n}PC_{il}(x,y)} \tag{5}$$

where n represents the number of place cells in the firing state.

$$a=\arg\max_{a}\left(\sum_{i=1}^{n}Q(s_i,a)\cdot act(s_i)\right) \tag{6}$$

$$Q(s_i,a)=act(s_i)\cdot\left(Q(s_i,a)+\Delta Q(s_i,a)\right)+\left(1-act(s_i)\right)\cdot Q(s_i,a) \tag{7}$$

$$\Delta Q(s_i,a)=\eta\cdot\left(r+\gamma\cdot\max_{a'}\left(\sum_{i=1}^{n}Q(s'_i,a')\cdot act(s'_i)\right)-Q(s_i,a)\right) \tag{8}$$

In contrast to the canonical Q-learning algorithm, our method takes all the place cells in the firing state into account as the input of the Q-learning process, and different place cells correspond to different Q values. When only one place cell is firing, $act(s_i)$ equals 1 and Eq.(7) is transformed into Eq.(3). Namely, the canonical Q-learning algorithm is a special case in our method.

For the firing place cells in each layer, the same method is employed to choose an appropriate action. **Fig. 4** gives the process for action selection according to the multi-scale place cell map in which the red circle indicates the place cells in a firing state and the gray shaded area indicates the firing activity. The color of the gray area is darker when the firing intensity of a place cell is greater. The arrow in the figure represents the action recommended in the current state. Through the integration of behavioral information given by the place cell

map in different scales, we can choose a reasonable action after a judgment and decision. Once an action a is executed, the Q values in each layer should be updated according to the action a in Eq.(7) and Eq.(8). After continuous iterative learning, the robot is able to integrate the behavioral information effectively and find an optimal route to the goal.

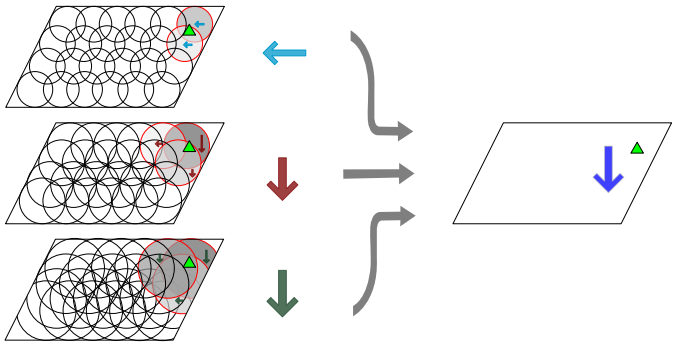

Fig. 4. The process of action selection for the multi-scale place cell map

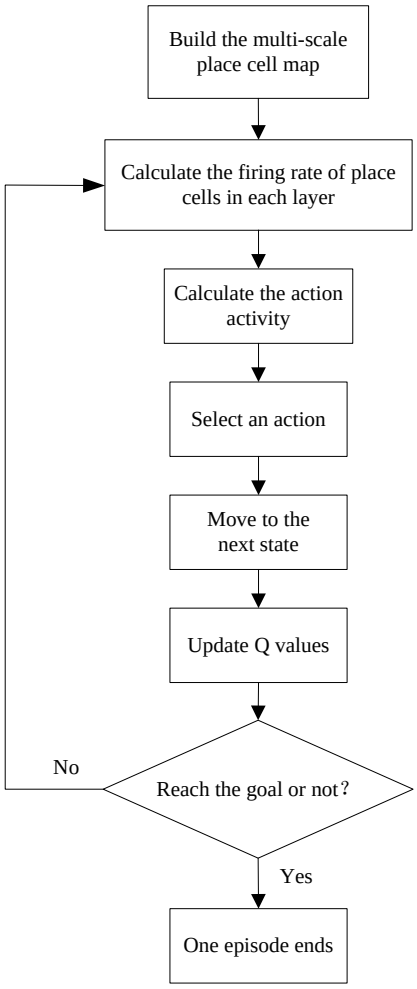

Fig. 5. A flow chart of the algorithm

Fig. 5 shows a flow chart of the algorithm in a single exploration. First, a multi-scale place cell map is built and the firing rate of the place cells in each layer is calculated as the input of the Q-learning algorithm for action selection. Then, a value for each possible action is computed and the most valued action is selected. Next, the robot moves to the next position and the Q values are updated according to Eq.(7). This step requires some judgment about whether the robot has reached the visible region of the goal. If it is, an exploration ends; if not, the robot continues to perform the same steps in a new state. After several exploration cycles, the robot can accumulate experiential knowledge and learn the appropriate navigation policy to move to the goal via an optimal route.

3. Performance Results and Analysis

To assess the performance of the method for completing the goal-directed navigation task, we analyze two aspects of the simulation in detail: one is a feasibility analysis from the perspective of the model implementation and the second is how a variety of parameters relevant in the model influence the positioning performance. All simulations are based on the Matlab R2010a platform.

3.1 Implementation of the model

First, the relevant parameters set in the simulation are introduced as follows:

(1) Spatial environment: It is supposed that the moving area of the robot is a square with a 100m×100m size.

(2) The starting point and the end point are, respectively, (15,15) and (85,90). The visible region for the goal is circular with a radius of 10m. When entering the region, the robot is considered to have reached the goal point.

(3) Setting the scale of the place cells: The multi-scale place cell map is constructed by using three different scales of the place cells in the simulation. The radius of the firing field is respectively set to 8m, 15m, and 25m. The place cell map in each layer is composed of one hundred place cells uniformly distributed.

(4) Action settings: The robot has three possible actions to choose from: rotate $\pi/4$ to the left and go forward 10m; go forward 10m; and rotate $\pi/4$ to the right and go forward 10m. All action directions are relative to the previous state. When the robot moves to the border, it will be given a reverse direction and choose a possible action anew. The velocity is 10m/s and the positioning period is 1s. The velocity and direction of the robot remains invariable within each positioning period.

(5) Q-learning algorithm parameters: The learning rate η and the discount factor γ are set to $\eta = 0.8$ and $\gamma = 0.9$, respectively.

Fig. 6 shows two sample paths from the starting point to the goal after one episode and ten episodes. An episode means that the agent finishes an exploration and finds the goal. The green triangle represents the starting point, the red pentacle represents the goal, and the red circle represents the visible region of the goal. In **Fig. 6(a)**, the simulated robot often moves randomly and needs many steps to reach the goal because there is no prior information about the environment in the first episode. Through exploring and learning the environment, the agent accumulates experiential knowledge continuously and improves its understanding of the goal's location. After ten episodes, the simulated robot is able to plan a short path to the goal as seen in **Fig. 6(b)**. **Table 1** shows the runtime for each episode in the method. It can be seen that the agent needs more time to explore the environment and look for the goal during the early

exploration. With an increasing number of episodes, the runtime for each episode decreases gradually. This means that the agent can gain more experiential knowledge about the environment and it becomes easier to find the goal after several episodes.

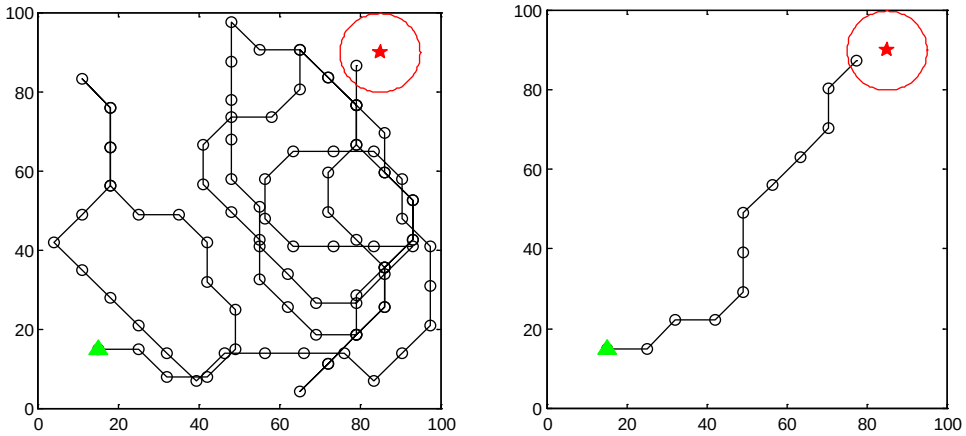

(a) One episode (b) After ten episodes

Fig. 6. Two sample paths, one after one episode and one after ten episodes

Table 1. Runtime comparison for each episode

Episode	1	2	3	4	5	6	7	8	9	10
Runtime(ms)	103	86	75	62	40	32	25	15	12	8

In order to illustrate the advantages of the multi-scale place cell map for goal-directed navigation, we compare the performance of the proposed methods with two other methods for goal-directed navigation. G-Q is a classical Q-learning algorithm based on grids, which divides the environment into many of the same grids where each grid represents a state of the Q-table. S-Q is an algorithm based on a single scale spatial representation, in which the space is represented by place cells with a single scale. In simulation, three different S-Q scale (S-Q-1, S-Q-2, S-Q-3) approaches are used for comparison where the scales are respectively set as $scale\ 1 = 8m$ (S-Q-1), $scale\ 2 = 15m$ (S-Q-2), $scale\ 3 = 25m$ (S-Q-3), and the other parameter settings are the same as above. M-Q is our proposed method, which uses a multi-scale place cell map to represent the position of the agent in the environment. The number of steps from the starting point to the goal position is considered the index which is used to evaluate the performance of the different methods.

Fig. 7 shows that the average number of steps is a function of the episode number. A step means that the simulated robot executes an action. An iteration represents the agent finishing 30 episodes. A hundred iterations are executed in simulation and each iteration provides the number of steps in each episode. Then we calculated the average steps in each episode over 100 iterations. As shown in the **Fig. 7**, the simulated robot can finish the goal-directed navigation task after several learning trials using all five approaches. With the number of episodes increasing gradually, the average number of steps decreases rapidly. When the episode number increases to a certain value, the average number of steps hardly changes,

which represents the simulated robot having found the shortest path to the destination. Compared with other four approaches, the M-Q method has a faster learning speed and is able to find an optimized path to the goal earlier under the same conditions. For example, after five episodes, the M-Q method only needs 18 steps to reach the goal while the other four methods need at least 39 steps.

Table 2 shows a runtime comparison of the different methods. We define the sum of the computational time from the initial state to the stable state in all 100 iterations as the runtime of the method. The stable state means that the number of steps from the starting point to the goal in the current episode is not greater than the number of steps in the next three episodes, which can be represented by Eq.(9). From **Table 2**, we know that the S-Q-3 method takes the most time and the M-Q method requires the least time, which is consistent with the results shown in **Fig. 7**. Compared to other methods, M-Q requires fewer episodes to reach a stable state and has a faster learning speed.

$$\begin{aligned} step(i) &\le step(i+1) \\ step(i) &\le step(i+2) \\ step(i) &\le step(i+3) \end{aligned} \tag{9}$$

where $step(i)$ represents the number of steps from the starting point to the goal in the ith episode.

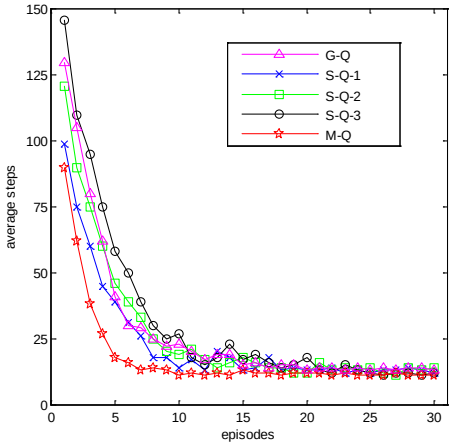

Fig. 7. The number of steps to reach the goal as a function of the episode number

Table 2. Runtime comparison of the different methods

Methods	G-Q	S-Q-1	S-Q-2	S-Q-3	M-Q
Runtime(s)	60.251	58.126	72.634	82.330	45.252

3.2 Performance in goal-directed navigation

This section focuses on how the change in the relevant parameters involved in the model has an impact on the performance of the M-Q method in completing the goal-directed

navigation. The parameter settings are the same as Section 3.1. **Fig. 8** shows the number of steps from the starting point to the goal under different learning rates such as $\eta = 0.8$, $\eta = 0.6$ and $\eta = 0.3$. The experiment under each episode is carried out 100 times and then the average steps are calculated to compare the performance when completing the goal-directed navigation task under different learning rates. From **Fig. 8**, we can see that the number of steps required to reach the goal is greater in the previous episodes. The average value and the variance of the steps decrease as the episode number increases. For comparison, the convergence speed becomes faster with the increase in learning rate, which means that the larger η has a faster learning potential to find the optimal path to the goal.

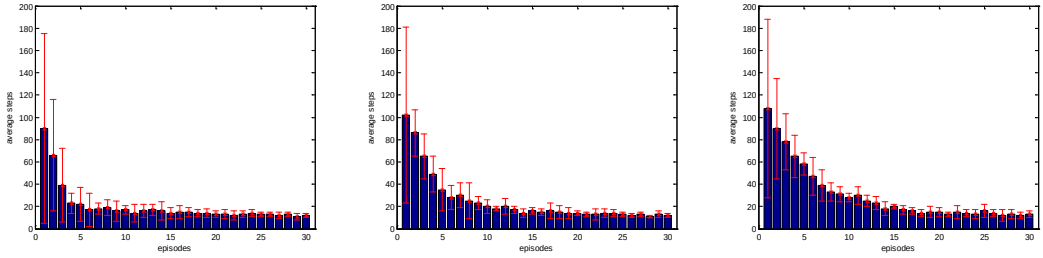

(a) $\eta = 0.8$ (b) $\eta = 0.6$ (c) $\eta = 0.3$

Fig. 8. The number of steps to reach the goal under different learning rates.

To test the multi-scale method performance in goal-directed navigation in a large space, the environment is expanded to a square region of 200m×200m, and other simulated parameters are the same as Section 3.1. In this circumstance, the place cell map in each layer is composed of 400 place cells, which are uniformly distributed. **Fig. 9** shows the path planning process in a large environment over 30 episodes. It can be seen that the number of steps that the agent required to reach the goal decreases as the number of episodes increases. After 30 episodes, the simulated robot is also able to plan an optimal route to the goal and succeeds in finishing the goal-directed navigation task by learning in the expanded space. Compared with a small environment, the method applied to large spaces requires more training trials.

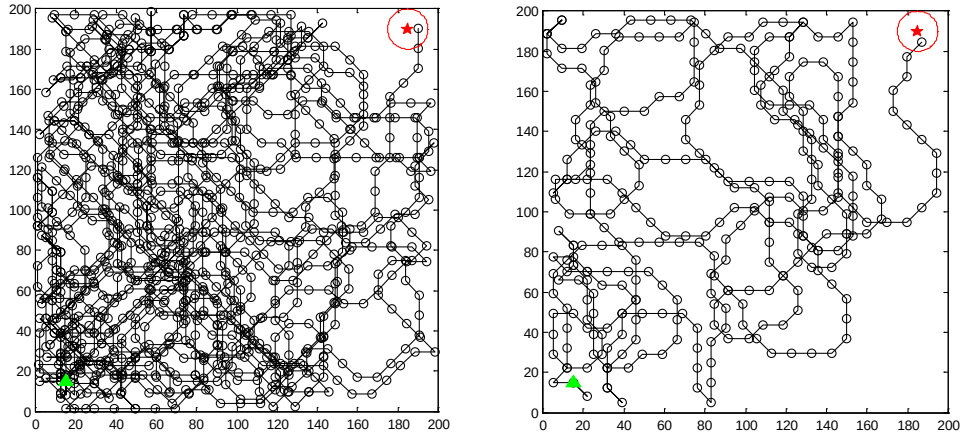

(a) One episode (b) After 7 episodes

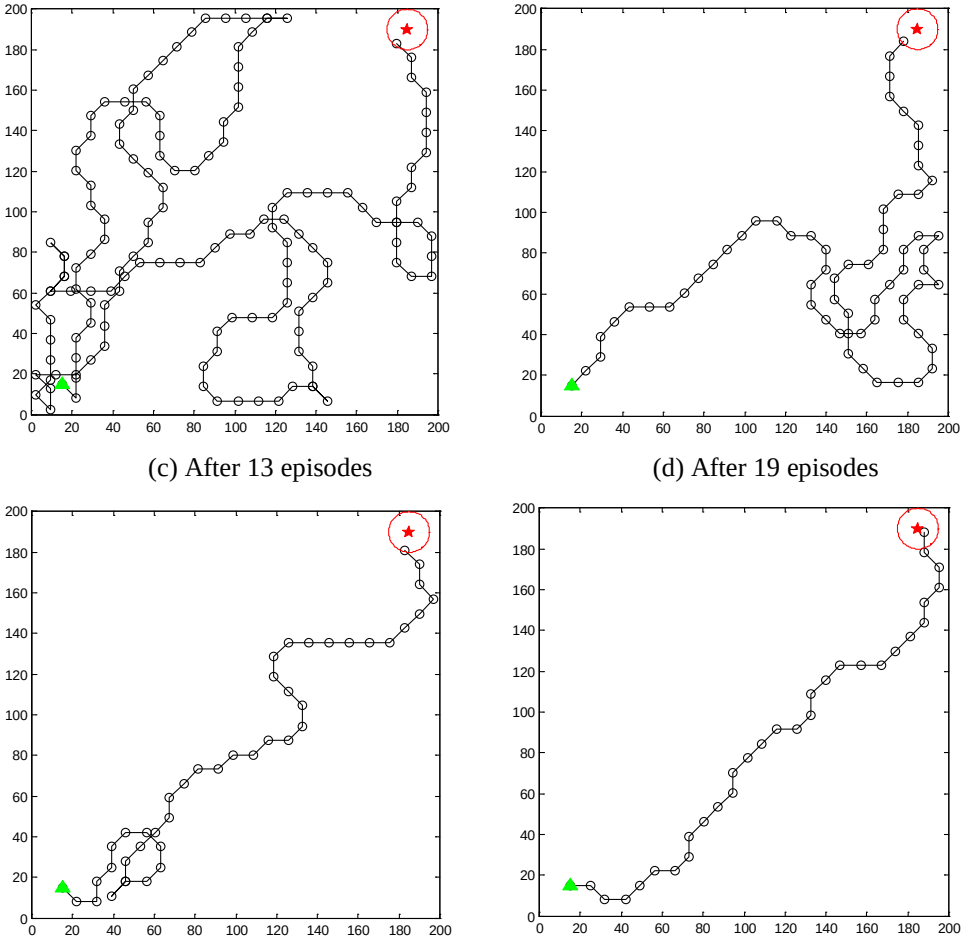

(c) After 13 episodes (d) After 19 episodes

(e) After 25 episodes (f) After 30 episodes

Fig. 9. Path planning process under different episodes

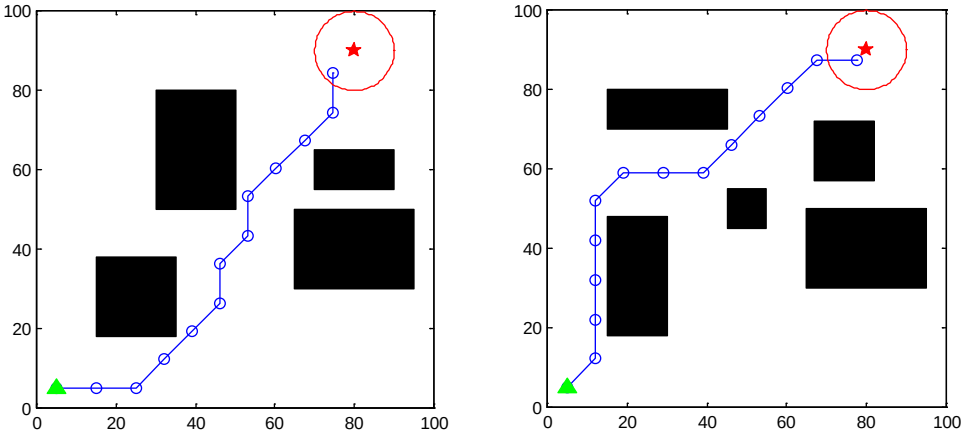

(a) Situation 1 (b) Situation 2

Fig. 10. The performance of the method in the environments with obstacles

Fig. 10 shows the performance of the proposed method in an environment with obstacles where the black rectangle represents the obstacle. The agent spends 30 episodes planning a short path in **Fig. 10(a)** and spends 50 episodes in **Fig. 10(b)**. The simulated robot can find a short path to the goal in both situations without colliding with the obstacles in the environment, which proves that the multi-scale method is also applicable to the cases where there are obstacles.

4. Conclusion

Considered a breakthrough discovery for human spatial cognition, the information processing mechanism of hippocampal place cells for spatial information are gaining more and more attention. Inspired by the phenomenon of multi-scale spatial representation in biology, a biologically inspired model based on a multi-scale spatial representation for goal-directed navigation is proposed in this paper. A reinforcement learning algorithm is used to combine the firing place cells with the actions so as to find a reasonable path to the goal after several episodes. The results of simulations show that the multi-scale spatial cognition model reveals a faster initial learning potential to find the hidden goal than the navigation strategy using G-Q and S-Q, and it also can complete the goal-directed navigation task in a large space and in the environments with obstacles. The method in this paper considers sensing, understanding, decision, and controlling as a whole process, which is not only in line with the biological basis for place cell firing, but it also improves the capability of the robot to deal with the integrated information much like the brain. Moreover, it also provides some reference for the development of bionic autonomous navigation.

In future work, we will focus on improving the details of the navigational model and testing the performance of the method on a hardware platform. The place cell firing is driven by the integration of idiothetic and allothetic information instead of the simulated firing model and then a reinforcement learning algorithm is adopted to complete a concrete navigation task. Additionally, we will pay more attention to the study on the information processing and transforming mechanism of head directed cells, speed cells, grid cells, and place cells so as to imitate the function of the brain for spatial navigation more realistically and further enhance the capability of intelligent autonomous navigation.

References

[1] A. Barrera, G. Tejera, M. Llofriu and A. Weitzenfeld, "Learning Spatial Localization: From Rat Studies to Computational Models of the Hippocampus," *Spatial Cognition & Computation: An Interdisciplinary Journal*, vol. 15, no. 1, pp. 27-59, 2015. Article (CrossRef Link)

[2] D. Derdikman and E.I. Moser, "A manifold of spatial maps in the brain," *Trends in Cognitive Sciences*, vol. 14, no. 12, pp. 561-569, 2010. Article (CrossRef Link)

[3] F. Chersi and N. Burgess, "The Cognitive Architecture of Spatial Navigation: Hippocampal and Striatal Contributions," *Neuron*, vol. 88, no. 1, pp. 64-77, 2015. Article (CrossRef Link)

[4] P.K. Raymond and T.R. Edmund, "A computational theory of hippocampal function, and tests of the theory: New developments," *Neuroscience and Biobehavioral Reviews*, vol. 48, pp. 92-147, 2015. Article (CrossRef Link)

[5] B.E. Pfeiffer and D.J. Foster, "Hippocampal place-cell sequences depict future paths to remembered goals," *Nature*, vol. 49, no. 7447, pp. 74-79, 2013. Article (CrossRef Link)

[6] E.C. Tolman, "Cognitive maps in rats and men," *Psychological Review*, vol. 55, no. 554, pp. 189-208, 1948. Article (CrossRef Link)

[7] J. O'Keefe and D.H. Conway, "Hippocampal place units in the freely moving rat: Why they fire where they fire," *Experimental Brain Research*, vol. 31, no. 4, pp. 573–590, 1978. Article (CrossRef Link)
[8] J. O'Keefe and J. DosLrovskv, "The Hippocampus as a spatial Map," *Brain Research*, vol. 34, no. 1, pp. 171-175, 1971. Article (CrossRef Link)
[9] J. O'Keefe and N. Burgess, "Geometric determinants of the place fields of hippocampal neurons," *Nature*, vol. 381, no. 6581, pp. 425-428, 1996. Article (CrossRef Link)
[10] J.S. Taube, R.U. Muller and J.B. Ranck, "Head-direction cells recorded from the postsubiculum in freely moving rats. I. Description and quantitative analysis," *Journal of Neuroscience*, vol. 10, no. 2, pp. 420-435, 1990. Article (CrossRef Link)
[11] L.M. Giocomo, T. Stensola, T. Bonnevie, T.V. Cauter, M.B. Moser and E.I. Moser, "Topography of head direction cells in medial entorhinal cortex," *Current Biology*, vol. 24, no. 3, pp. 252-262, 2014. Article (CrossRef Link)
[12] T. Hafting, M. Fyhn, S. Molden, M.B. Moser and E.I. Moser, "Microstructure of a spatial map in the entorhinal cortex," *Nature*, vol. 436, no. 7052, pp. 801-806, 2005. Article (CrossRef Link)
[13] E.I. Moser, Y. Roudi, M.P. Witter, C. Kentros, T. Bonhoeffer and M.B. Moser, "Grid cells and cortical representation," *Nature Reviews Neuroscience*, vol. 15, no. 7, pp. 466-481, 2014. Article (CrossRef Link)
[14] T. Solstad, C.N. Boccara, E. Kropff, M.B. Moser and E.I. Moser, "Representation of geometric borders in the entorhinal cortex," *Science*, vol. 322, no. 5909, pp. 1865-1868, 2008. Article (CrossRef Link)
[15] E. Kropff, J.E. Carmichael, M.B. Moser and E.I. Moser, "Speed cells in the medial entorhinal cortex," *Nature*, vol. 523, no. 7561, pp. 419-424, 2015. Article (CrossRef Link)
[16] T. Wolbers, "Spatial Navigation," *International Encyclopedia of the Social & Behavioral Sciences*, vol. 23, pp. 161-171, 2015. Article (CrossRef Link)
[17] S. Grossberg, "From brain synapses to systems for learning and memory: Object recognition, spatial navigation, timed conditioning, and movement control," *Brain Research*, vol. 6121, pp. 270-293, 2015. Article (CrossRef Link)
[18] R.M. Tavares, A. Mendelsohn, Y. Grossman, C.H. Williams, M. Shapiro, Y. Trope and D. Schiller, "A Map for Social Navigation in the Human Brain," *Neuron*, vol. 87, no. 1, pp. 231-243, 2015. Article (CrossRef Link)
[19] I. Kostavelis, K. Charalampous, A. Gasteratos and J.K. Tsotsos, "Robot navigation via spatial and temporal coherent semantic maps," *Engineering Applications of Artificial Intelligence*, vol. 48, pp. 173-187, 2016. Article (CrossRef Link)
[20] Q. Zhu, R.B. Wang and Z.Y. Wang, "A cognitive map model based on spatial and goal-oriented mental exploration in rodents," *Behavioural Brain Research*, vol. 256, no. 11, pp. 128-139, 2013. Article (CrossRef Link)
[21] D. Bush, C. Barry, D. Manson and N. Burgess, "Using Grid Cells for Navigation," *Neuron*, vol. 87, no. 3, pp. 507-520, 2015. Article (CrossRef Link)
[22] H.J. Spiers and C. Barry, "Neural systems supporting navigation," *Current Opinion in Behavioral Sciences*, vol. 1, no. 1, pp. 47-55, 2015. Article (CrossRef Link)
[23] U.M. Erdem, M.E. Hasselmo, "A goal-directed spatial navigation model using forward trajectory planning based on grid cells," *European Journal of Neuroscience*, vol. 35, no. 6, pp. 916-931, 2012. Article (CrossRef Link)
[24] M.G. Sagiv, L. Las, Y. Yovel and N. Ulanovsky, "Spatial cognition in bats and rats: from sensory acquisition to multiscale maps and navigation," *Nature Reviews Neuroscience*, vol. 16, no. 2, pp. 94-108, 2015. Article (CrossRef Link)
[25] A.T. Keinath, M.E. Wang, E.G. Wann, R.K. Yuan, J.T. Dudman and I. A. Muzzio, "Precise spatial coding is preserved along the longitudinal hippocampal axis," *Hippocampus*, vol. 24, no. 12, pp. 1533-1548, 2014. Article (CrossRef Link)
[26] U.M. Erdem, M.J. Milford and M.E. Hasselmo, "A hierarchical model of goal directed navigation selects trajectories in a visual environment," *Neurobiology of Learning and Memory*, vol. 117, pp. 109-121, 2015. Article (CrossRef Link)

[27] Z. Chen, S. Lowry, A. Jacobson, M.E. Hasselmo and M.J. Milford, "Bio-inspired homogeneous multi-scale place recognition," *Neural Networks*, vol. 72, pp. 48-61, 2015. Article (CrossRef Link)
[28] L.L. Long, J.G. Bunce and J.J. Chrobak, "Theta variation and spatiotemporal scaling along the septotemporal axis of the hippocampus," *Frontiers in Systems Neuroscience*, vol. 9, no. 37, pp. 1-14, 2015. Article (CrossRef Link)
[29] R.J. Robitsek, J.A. White and H. Eichenbaum, "Place cell activation predicts subsequent memory," *Behavioural Brain Research*, vol. 254, no. 4, pp.65-72, 2013. Article (CrossRef Link)
[30] A. Konar, I.G. Chakraborty, J.S. Sapam, C.J. Lakhmi and K.N. Atulya, "A Deterministic Improved Q-Learning for Path Planning of a Mobile Robot," *IEEE Transactions on Systems, Man, and Cybernetics: Systems*, vol. 43, no. 5, pp. 1141-1153, 2015. Article (CrossRef Link)
[31] N. Cuperlier, M. Quoy and P. Gaussier, "Navigation and Planning in an Unknown Environment Using Vision and a Cognitive Map," *European Robotics Symposium*, vol. 22, pp. 129-142, 2006. Article (CrossRef Link)
[32] P. Giovanni, A.A. Matthijs, C.S. Lansink and M.A. C. Pennartz, "Internally generated sequences in learning and executing goal-directed behavior," *Trends in Cognitive Sciences*, vol. 18, no. 12, pp. 647-657, 2014. Article (CrossRef Link)

Weilong Li received his M.Sc. degree in Communication and Information System from Air Force Engineering University, Xi'an, Shaanxi, P.R. China, in 2013. He is currently pursuing a Ph.D. degree at Information and Navigation College, Air Force Engineering University. His main research directions include intelligent and autonomous navigation, biological computer vision.

Dewei Wu is a professor and Ph.D. supervisor at Information and Navigation College, Air Force Engineering University. He received his M.Sc. degree in Military Equipment Science from Air Force Engineering University in 2001 and received his Ph.D. degree in System Engineering from Northwestern Polytechnical University, Xi'an, Shaanxi, P.R. China, in 2005. His main research directions include navigation positioning theory, technology and application, intelligent and autonomous navigation, quantum navigation. He is a senior member of the China Institute of Electronics and serves as an expert committee member in the Electronics Institute of Shaanxi Province.

Jia Du received her M.Sc. degree from Xi'an Communications Institute in 2008. She is currently pursuing a Ph.D. degree at Information and Navigation College, Air Force Engineering University. Her main research directions include intelligent and autonomous navigation, biological trajectory planning.

Yang Zhou received his M.Sc. degree from Air Force Engineering University in 2014. He is currently pursuing a Ph.D. degree at Information and Navigation College, Air Force Engineering University. His main research directions include intelligent and autonomous navigation, computer vision.